10-5

Efficient Demagnetizing Field Calculation for Disconnected Complex Geometries in STT-MRAM Cells

Johannes Ender
Christian Doppler Laboratory for NovoMemLog at the Institute for Microelectronics TU Wien
Vienna, Austria
ender@iue.tuwien.ac.at

Mohamed Mohamedou
Christian Doppler Laboratory for NovoMemLog at the Institute for Microelectronics TU Wien
Vienna, Austria
mohamedou@iue.tuwien.ac.at

Simone Fiorentini
Christian Doppler Laboratory for NovoMemLog at the Institute for Microelectronics TU Wien
Vienna, Austria
fiorentini@iue.tuwien.ac.at

Roberto Orio
Institute for Microelectronics TU Wien
Vienna, Austria
orio@iue.tuwien.ac.at

Siegfried Selberherr
Institute for Microelectronics TU Wien
Vienna, Austria
selberherr@iue.tuwien.ac.at

Wolfgang Goes
Silvaco Europe Ltd
Cambridge, United Kingdom
wolfgang.goes@silvaco.com

Viktor Sverdlov
Christian Doppler Laboratory for NovoMemLog at the Institute for Microelectronics TU Wien
Vienna, Austria
sverdlov@iue.tuwien.ac.at

***Abstract*—Micromagnetic simulations of MRAM cells are a computationally demanding task. Different methods exist to handle the computational complexity of the demagnetizing field, the most expensive magnetic field contribution. In this work we show how the demagnetizing field can efficiently be calculated in complex memory structures and how this procedure can be further used to simulate spin-transfer torque switching in magnetic tunnel junctions.**

Keywords—Micromagnetics, LLG, spin-transfer torque, MRAM, demagnetizing field

I. Introduction

Spin-transfer torque magnetic random access memory (STT-MRAM) is an emerging non-volatile memory compatible with CMOS technology rapidly conquering the market. STT-MRAM possesses an endurance higher than flash memory, and it is suitable for both stand-alone and embedded applications. STT-MRAM is fast and its access time can be tuned in a broad range. This positions STT-MRAM as a universal memory capable to replace both static random access memory and flash memory [1]-[7].

Magnetic tunnel junctions (MTJ) are the basic means to store the information of a single bit and lie at the heart of every MRAM cell. As information has to be read and written many times and the magnetization in the MTJ undergoes frequent changes, the dynamic behavior of this process is of great interest. Here, micromagnetic simulations provide deeper insight and many simulation tools have been developed for this purpose in recent years [8].

Our aim is to develop a simulation tool based on the finite element method (FEM) in order to efficiently perform magnetization dynamics simulations of spintronic devices. The focus in this work lies on the efficient calculation of the demagnetizing field, for which special means are required to prevent the excessive use of memory and computation time.

II. The Computational Challenges

Calculating magnetization dynamics in the magnetic layers of an STT memory cell involves the solution of the extended Landau-Lifshitz-Gilbert (LLG) equation

$$\frac{\partial \mathbf{m}}{\partial t} = -\gamma\mu_0 \mathbf{m} \times \mathbf{H}_{\text{eff}} + \alpha \mathbf{m} \times \frac{\partial \mathbf{m}}{\partial t} + \frac{1}{M_s}\mathbf{T}_S \,, \tag{1}$$

where $\mathbf{m}=\mathbf{M}/M_S$ is the position-dependent magnetization normalized by the saturation magnetization M_S, γ is the gyromagnetic ratio, μ_0 is the vacuum permeability, α is the Gilbert damping constant, $\mathbf{H}_{\text{eff}}$ is the effective magnetic field, and $\mathbf{T}_S$ is the spin-torque exerted by a spin-polarized current flowing through the memory cell.

In a FEM discretization, the computationally most demanding contribution of the effective field is the demagnetizing field $\mathbf{H}_d$, which describes the long-range dipole interaction of the magnetic moments. To compute the demagnetizing field by FEM, it is convenient to introduce a scalar magnetic potential u defining

$$\mathbf{H}_d = -\nabla u \tag{2}$$

with u being the solution of the following Poisson equation:

$$\nabla^2 u = \nabla \cdot \mathbf{M} \tag{3}$$

As the potential $u(\mathbf{x})$ slowly decays to zero as $|\mathbf{x}| \to \infty$, a large computational domain surrounding the magnetic material is required in a FEM simulation to accurately describe this behavior. Various solutions to this so-called open boundary problem have been suggested [8]-[11]. The

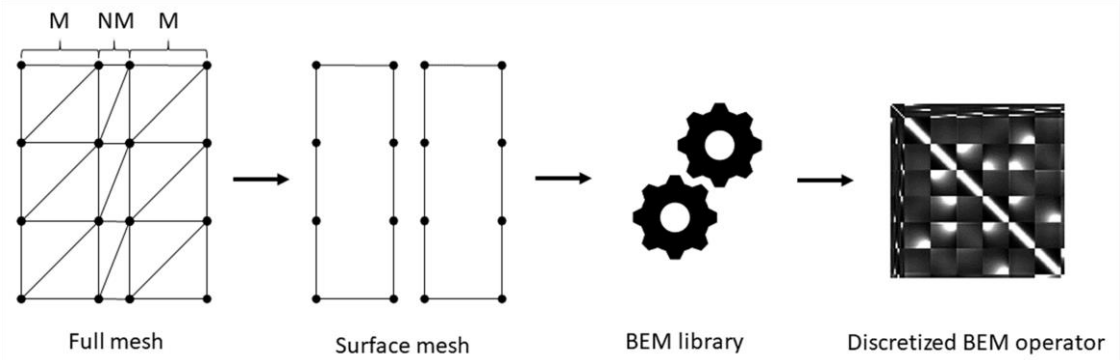

Figure 1: Depiction of the process for discretizing a boundary integral operator, which considers the interaction between disconnected magnetic parts.

truncation of the external computational domain surrounding the magnetic material at a certain distance is usually called truncation approach. As computational efficiency is desired, the external domain cannot be made too large in order to keep the number of degrees of freedom small. An external domain of around five times larger than the magnetic domain has shown to be an acceptable trade-off between computational efficiency and accuracy [12].

To achieve high accuracy and reduce the computational costs, a hybrid approach, where the finite element method is coupled to the boundary element method (hybrid FEM-BEM), is employed to restrict computation to the magnetic domain [13]. Here, the potential is split into two parts u_1 and u_2, calculated by solving a Poisson and a Laplace equation with respect to the corresponding boundary conditions. The potentials u_1 and u_2 are related by the integral over the boundary $\partial\Omega$ of the magnetic domain [13].

$$u_2 = \int_{\partial\Omega} u_1 \frac{\partial}{\partial \mathbf{n}} \frac{1}{|\mathbf{x}-\mathbf{x}'|} d^2\mathbf{x} \qquad (4)$$

This relation in its discretized form reduces to the following matrix-vector multiplication:

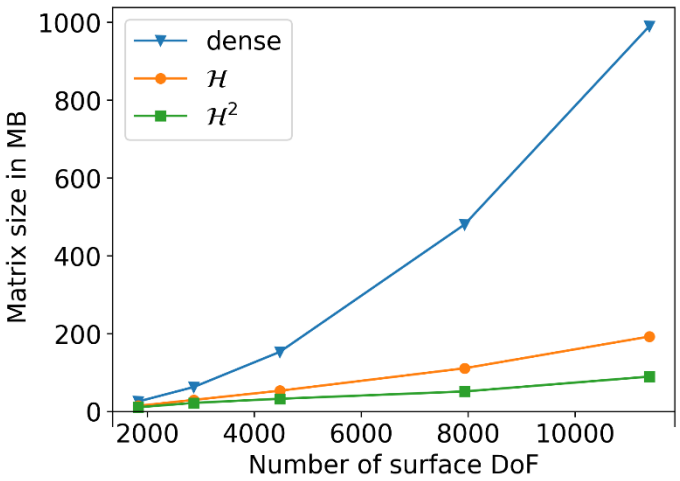

Figure 2: Comparison of the memory consumption of the uncompressed boundary operator matrix and when applying H and H^2 matrix compression algorithms, respectively.

$$u_2 = \mathbf{B} \cdot u_1 \qquad (5)$$

Using (5), u_2 is evaluated at the boundary and set as Dirichlet boundary condition for the Laplace equation. Despite the benefit of the hybrid FEM-BEM method to drastically reduce the size of the computational domain, it comes at the cost of having to deal with dense matrices, arising from the discretization of the boundary operator **B** in (5). To reduce the high memory demands, matrix compression algorithms are applied [14]. So-called hierarchical matrix compression algorithms approximate the original matrix by hierarchically decomposing it into low-rank submatrices, which are then represented as a factorization of two matrices. These compression algorithms

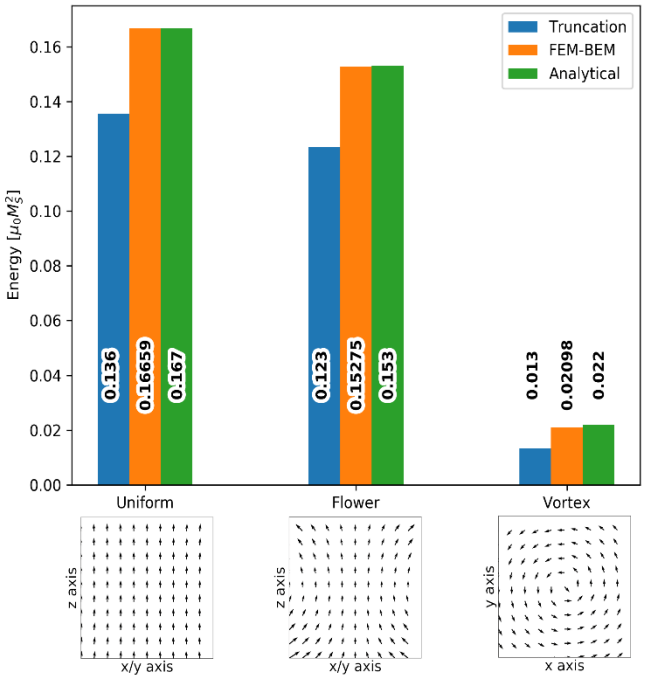

Figure 3: Comparison of the demagnetizing energy of a unit cube with different magnetization configurations calculated with the truncation approach and the hybrid FEM-BEM approach.

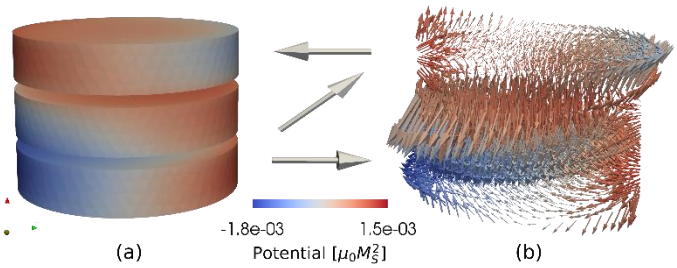

Figure 4: Magnetic potential (a) and demagnetizing field (b) calculated for a three-layer structure. The arrows indicate the magnetization orientation in the respective layers. The color-coding in both figures indicates the magnetic potential value.

can significantly reduce the memory requirements of the simulation, as can be seen in Figure 2.

We implemented the demagnetizing field calculations into a micromagnetic simulation environment written in C++, which uses finite elements to solve (1) in STT-MRAM devices. In order to enhance the performance and accuracy, the open-source third party dependencies of the tool are the FEM library MFEM [15] and H2Lib [16]. The latter library contains matrix compression algorithms and basic BEM functionality.

Simulating magnetization dynamics in an STT-MRAM cell requires the calculation of the demagnetizing field of more complex magnetic structures. These consist of multiple disjoint magnetic layers whose stray fields act on each other. The boundary operator must be set up properly to deal with magnetic regions only for the hybrid FEM-BEM approach. In order to do this, we implemented the strategy depicted in Figure 1, where a simplified two-dimensional scenario is shown. As it is usually found in magnetic tunnel junctions, the three-layered structure consists of two magnetic (M) layers sandwiching a non-magnetic (NM) layer. In a first step the surface mesh of the magnetic regions is extracted from the full volume mesh. Treating this as a single mesh - even if disconnected – it is subsequently fed into the BEM library that performs the discretization of the boundary integral operator (5). This densely populated matrix incorporates the interaction between the magnetic layers and is then used in the calculation of the values of u_2. The procedure of generating the boundary operator **B** is computationally demanding, but must be performed only once, as it solely depends on the geometry of the structure to be calculated.

TABLE I: SIMULATION PARAMETERS

Parameter	***Value***
Gilbert damping, α	0.02
Gyromagnetic ratio, γ	$1.76 \cdot 10^{11}$ rad s^{-1} T^{-1}
Vacuum permeability, μ_0	$4\pi \cdot 10^{-7}$ H m^{-1}
Saturation magnetization, M_S	$8 \cdot 10^{5}$ A m^{-1}
Exchange constant, A	$1.3 \cdot 10^{-11}$ J m^{-1}
Anisotropy constant, K	$2 \cdot 10^{5}$ J m^{-3}

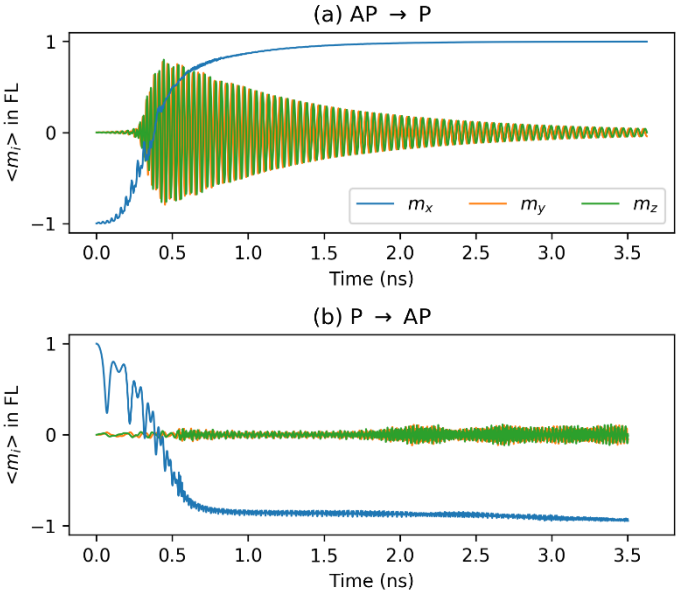

Figure 5: Average of the magnetization components during the switching process of a perpendicularly magnetized STT-MRAM cell from the (a) anti-parallel (AP) to parallel (P) configuration and from the (b) parallel to the anti-parallel configuration. The x direction is the direction of perpendicular magnetic anisotropy.

III. RESULTS

Using a set of micromagnetic standard problems [17], we verified the correctness of our results for the demagnetizing field calculation and can now confirm that the hybrid FEM-BEM approach is superior to the truncation approach with respect to accuracy, as can be seen in Figure 3. Here, the demagnetizing energy of a unit cube with several initial magnetizations, computed with the two above-mentioned approaches, was compared to the analytical value. Cross-sections of the different magnetization scenarios can be seen on the bottom of Figure 3. A uniform magnetization as well as a so-called flower state and a vortex-like magnetization are compared. While the relative error for the truncation approach ranges from around 19% in the uniform and flower scenario to up to 39% in the vortex scenario, the hybrid FEM-BEM approach on the other hand achieves a relative error of below 1% for the first two scenarios and remains under 5% for the vortex scenario.

Figure 4 shows the result obtained for computing the magnetic potential (Figure 4a) and the demagnetizing field (Figure 4b) for a magnetic structure consisting of three disjoint magnetic layers with the magnetization in the respective layers indicated by the arrows in the middle. Without interaction, the potential would be varying linearly along the direction of the magnetization in the corresponding layer. When applying the strategy depicted in Figure 1 this is not the case and the magnetic potential is shifted due to the different orientations of the magnetization in the three layers and their mutual interaction.

Applying the developed technique for calculating the demagnetizing field, we successfully simulated the switching of a perpendicularly magnetized STT-MRAM cell.

The magnetization in the reference layer is fixed in the positive x direction and the contributions to the effective magnetic field $\mathbf{H}_{\text{eff}}$ include the exchange field, the anisotropy field and the demagnetizing field. By applying a current through the MTJ a switching from an anti-parallel (AP) to a parallel (P) configuration was simulated as well as switching from P to AP. Figure 5 shows the average of the magnetization components in the free layer (FL). The parameters used for the simulations can be seen in Table I.

IV. Conclusion

In this work we presented how, by the use of open-source libraries, efficient micromagnetic simulations can be carried out. Through a drastic reduction of the computational domain and compression of large, dense matrices, the overall performance of the demagnetizing field calculation can be optimized. Results were compared with reference problems for uniform and non-uniform magnetization and a strategy was demonstrated that enables the computation of the demagnetizing field in complex geometries with disconnected magnetic regions. In addition, results of a simulation showing the switching between the two states of an STT-MRAM cell were presented.

Acknowledgment

This work was supported by the *Austrian Federal Ministry for Digital and Economic Affairs* and the *National Foundation for Research, Technology and Development.*

References

[1] D. Apalkov, B. Dieny, J. M. Slaughter, "Magneto-resistive Random Access Memory," *Proceedings of the IEEE*, *104*(10), pp. 1796-1830, 2016.

[2] S. Aggarwal, H. Almasi, M. DeHerrera, B. Hughes, S. Ikegawa *et al.*, "Demonstration of a Reliable 1 Gb Standalone Spin-Transfer Torque MRAM for Industrial Applications," *Proceedings of the IEDM*, pp. 2.1.1-2.1.4, 2019.

[3] K. Lee, J. H. Bak, Y. J. Kim, C. K. Kim, A. Antonyan *et al.*, "1Gbit High Density Embedded STT-MRAM in 28nm FDSOI Technology," *Proceedings of the IEDM*, pp. 2.2.1-2.2.4, 2019.

[4] V. B. Naik, K. Lee, K. Yamane, R. Chao, J. Kwon *et al.*, "Manufacturable 22nm FD-SOI Embedded MRAM Technology for Industrial-Grade MCU and IOT Applications," *Proceedings of the IEDM*, pp. 2.3.1-2.3.4, 2019.

[5] J. G. Alzate, U. Arslan, P. Bai, J. Brockman, Y. J. Chen *et al.*, "2 MB Array-Level Demonstration of STT-MRAM Process and Performance Towards L4 Cache Applications," *Proceedings of the IEDM*, pp. 2.4.1-2.4.4, 2019.

[6] G. Hu, J. J. Nowak, M. G. Gottwald, S. L. Brown, B. Doris *et al.*, "Spin-Transfer Torque MRAM with Reliable 2 ns Writing for Last Level Cache Applications," *Proceedings of the IEDM*, pp. 2.6.1-2.6.4, 2019.

[7] W. J. Gallagher, E. Chien, T. W. Chiang, J. C. Huang, M. C. Shih *et al.*, "22nm STT-MRAM for Reflow and Automotive Uses with High Yield, Reliability, and Magnetic Immunity and with Performance and Shielding Options," *Proceedings of the IEDM*, pp. 2.7.1-2.7.4, 2019.

[8] J. Leliaert, J. Mulkers, "Tomorrow's Micromagnetic Simulations," *Journal of Applied Physics*, *125*(18), p. 180901, 2019.

[9] J. Imhoff, G. Meunier, X. Brunotte, and J. Sabonnadiere, "An Original Solution for Unbounded Electromagnetic 2d- and 3d-Problems Throughout the Finite Element Method," *IEEE Transactions on Magnetics*, *26*(5), pp. 1659–1661, 1990.

[10] X. Brunotte, G. Meunier, and J.-F. Imhoff, "Finite Element Modeling of Unbounded Problems using Transformations: a Rigorous, Powerful and Easy Solution," *IEEE Transactions on Magnetics*, *28*(2), pp. 1663–1666, 1992.

[11] F. Henrotte, B. Meys, H. Hedia, P. Dular, and W. Legros, "Finite Element Modelling with Transformation Techniques," *IEEE transactions on magnetics*, *35*(3), pp. 1434-1437, 1999.

[12] Q. Chen, A. Konrad, "A Review of Finite Element Open Boundary Techniques for Static and Quasi-Static Electromagnetic Field Problems," *IEEE Transactions on Magnetics*, *33*(1), pp. 663-676, 1997.

[13] D. R. Fredkin, T. R. Koehler, "Hybrid Method for Computing Demagnetizing Fields," *IEEE Transactions on Magnetics*, *26*(2), pp. 415-417, 1990.

[14] N. Popović, D. Praetorius, "Applications of H-Matrix Techniques in Micromagnetics," *Computing*, *74*(3), pp. 177-204, 2005.

[15] T. Kolev, V. Dobrev, "MFEM: Modular Finite Element Methods Library," http://mfem.org, 2010.

[16] N. Albrecht, C. Börst, D. Boysen, S. Christophersen, S. Börm, "H2Lib," http://www.h2lib.org, 2016.

[17] C. Abert, L. Exl, G. Selke, A. Drews, T. Schrefl, "Numerical Methods for the Stray-Field Calculation: A Comparison of Recently Developed Algorithms," *Journal of Magnetism and Magnetic Materials*, *326*, pp. 176-185, 2013.